ORIGINAL PAPER

Divalent metal ions tune the self-splicing reaction of the yeast mitochondrial group II intron Sc.ai5γ

Michèle C. Erat · Roland K. O. Sigel

Abstract Group II introns are large ribozymes, consisting of six functionally distinct domains that assemble in the presence of Mg^{2+} to the active structure catalyzing a variety of reactions. The first step of intron splicing is well characterized by a Michaelis–Menten-type cleavage reaction using a two-piece group II intron: the substrate RNA, the 5′-exon covalently linked to domains 1, 2, and 3, is cleaved upon addition of domain 5 acting as a catalyst. Here we investigate the effect of Ca^{2+}, Mn^{2+}, Ni^{2+}, Zn^{2+}, Cd^{2+}, Pb^{2+}, and $[Co(NH_3)_6]^{3+}$ on the first step of splicing of the *Saccharomyces cerevisiae* mitochondrial group II intron Sc.ai5γ. We find that this group II intron is very sensitive to the presence of divalent metal ions other than Mg^{2+}. For example, the presence of only 5% Ca^{2+} relative to Mg^{2+} results in a decrease in the maximal turnover rate k_{cat} by 50%. Ca^{2+} thereby has a twofold effect: this metal ion interferes initially with folding, but then also competes directly with Mg^{2+} in the folded state, the latter being indicative of at least one specific Ca^{2+} binding pocket interfering directly with catalysis. Similar results are obtained with Mn^{2+}, Cd^{2+}, and $[Co(NH_3)_6]^{3+}$. Ni^{2+} is a much more powerful inhibitor and the presence of either Zn^{2+} or Pb^{2+} leads to rapid degradation of the RNA. These results show a surprising sensitivity of such a large multidomain RNA on trace amounts of cations other than Mg^{2+} and raises the question of biological relevance at least in the case of Ca^{2+}.

Introduction

Natural ribozymes, i.e., catalytic RNAs, mostly carry out phosphodiester cleavage or phosphoryl transfer reactions [1], but they can potentially be engineered to assume many more functions [2, 3]. The simplest true ribozyme described to date is the trinucleotide UUU, which cleaves the GAAA tetranucleotide specifically between G and A in the presence of Mn^{2+} [4]. This minimal catalytically active structure provides evidence that even very simple RNAs can direct specific hydrolysis, using metal ions as their cofactor.

No RNA molecule can exhibit its function in the absence of metal ions. Divalent metal ions are crucial to achieve the folded state and are often implicated to also participate directly in catalysis in some way [5]. Among the small ribozymes, a few can also be activated in the presence of molar concentrations of monovalent ions only [6–8]. The smallest among these ribozymes, the hammerhead ribozyme, was identified on the positive strand of the satellite RNA from the tobacco ringspot virus. Like in all ribozymes, Mg^{2+} is considered to be the natural cofactor, but interestingly the hammerhead ribozyme reaches its highest activity in the presence of Mn^{2+} [9]. Co^{2+}, Ni^{2+}, Zn^{2+}, and Cd^{2+} also lead to higher in vitro cleavage rates than Mg^{2+} [9, 10]. Obviously, the hammerhead ribozyme is rather flexible in its usage of divalent metal ions, as is additionally illustrated by its activity in the presence of Ca^{2+}, Sr^{2+}, and Ba^{2+}. Instead, the hairpin ribozyme that is found on the negative strand of the same virus and displays the same overall mechanism only shows efficient catalysis

M. C. Erat · R. K. O. Sigel (✉)
Institute of Inorganic Chemistry,
University of Zurich,
8057 Zurich, Switzerland
e-mail: roland.sigel@aci.uzh.ch

in the presence of Mg^{2+}, Ca^{2+}, and Sr^{2+}, but not with Mn^{2+} and Co^{2+} [11].

From the abovementioned examples it is already clear that ribozymes are very sensitive to the presence of divalent metal ions other than Mg^{2+}. This specific recognition must be based on charge, size, and coordination preferences of these metal ions and has been exploited in recent years by engineering in vitro selected DNAzymes specific to Mg^{2+}, Ca^{2+}, Zn^{2+} or even Pb^{2+} [12–16]. The metal ion specificity can thereby also be switched from Mg^{2+} to, e.g., Ca^{2+}, as has been shown with the *Tetrahymena* [17, 18] as well as the *Azoarcus* [19] group I introns, which are usually only active in the presence of either Mg^{2+} or Mn^{2+}.

Group II introns are the largest naturally occurring ribozymes apart from the ribosome, consisting of six domains projecting from a central wheel (Fig. 1). All group II introns investigated until today require Mg^{2+} for activity, although the amount needed differs up to a factor of 1,000 depending on the origin of the intron [20–22]. Folding and domain assembly is in all cases induced by the addition of Mg^{2+}. Recent studies showed that in the D135 ribozyme derived from the *Saccharomyces cerevisiae* group II intron *Sc*.ai5γ, the κ–ζ region within domain 1 (D1) constitutes the nucleation element for folding at low millimolar Mg^{2+} concentration, guiding the D1 scaffold to the correct architecture [23, 24]. At higher Mg^{2+} concentrations, the other domains then subsequently bind to D1, with domain 5 (D5) coming last and completing the catalytic core [25].

Although Mg^{2+} is believed to be the natural metal ion cofactor of group II introns and to be involved directly in catalysis [26, 27], many other kinds of metal ions have been applied for different purposes: Mn^{2+} and Zn^{2+} [28], as well as lanthanide(III) and Pb^{2+} ions revealed metal ion binding sites [23, 29, 30], and Mn^{2+}, Zn^{2+}, and Cd^{2+} were used in nucleotide analogue interference mapping/suppression (NAIH/NAIS) studies to reveal tertiary contacts as well as to identify coordinating atoms within the catalytic center via thio-rescue experiments [26, 31–34]. It is obvious that all of these ions differ in their intrinsic coordinating properties [35], and their binding pattern might also be influenced differently by changes in the electric permittivity within the folded RNA structure [36]. However, despite their general usage, the effect of these different metal ions on splicing has to the best of our knowledge not yet been quantified. In addition, in the light of the above-described accelerating effect of metal ions other than Mg^{2+} on the hammerhead function, also the question arises of whether such an effect is also seen in the case of group II introns, and whether there is a possible biological relevance.

Here, we apply a well-characterized bipartite system consisting of the 5′-exon covalently linked to D1 and
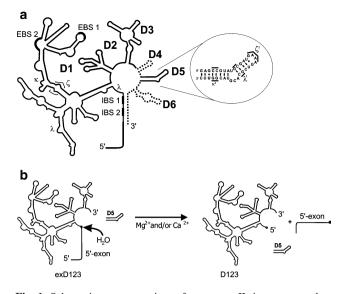

Fig. 1 Schematic representation of a group II intron secondary structure together with the *trans*-splicing assay used. **a** The six functionally distinct domains of the group II intron *Sc*.ai5γ from the *Saccharomyces cerevisiae* mitochondrial *cox1* gene with catalytic domain 5 (*D5*) enlarged are shown. The three tertiary contacts between domain 1 (*D1*) and D5 (κ–κ', λ–λ', ζ–ζ') and the exon/intron binding interactions (EBS1/IBS1 and EBS2/IBS2), which are responsible for proper alignment of the splice site in the catalytic core, are indicated. **b** The single-turnover *trans*-cleavage assay: the substrate (*exD123*) consists of the last 293 nucleotides from the 5′-exon, including the intron binding sites IBS1 and IBS2, the 5′-splice site as well as D1 and domains 2 and 3 from the intron *Sc*.ai5γ (710 nucleotides). The catalytic D5 flanked by 22 nucleotides was added in *trans*. A solvent water molecule acts as the nucleophile in the first step of splicing (see also "Materials and methods" and the text). The reaction is induced by addition of Mg^{2+} ions (or Mg^{2+}-to-Ca^{2+} ratios) to yield two products, D123 and the cleaved-off 5′-exon. D5 as a real catalyst is left unchanged during the reaction

domains 2 and 3 (exD123) of *Sc*.ai5γ as a substrate and D5 added in *trans* acting as a catalyst (Fig. 1) [37, 38]. This setup has been shown to reliably mimic the first step of splicing and to follow Michaelis–Menten kinetics [37]. We show that in the presence of 90 mM Mg^{2+}, 10 mM Ca^{2+}, Mn^{2+}, Ni^{2+}, Zn^{2+}, Cd^{2+}, Pb^{2+}, or $[Co(NH_3)_6]^{3+}$ leads to a substantial inhibition of the first step of splicing, if not even to unspecific degradation of the RNA. For example, the reaction rate is reduced to half by Ca^{2+} in the presence of 100-fold excess of Mg^{2+}. This strong inhibition is surprising as Ca^{2+} is placed below Mg^{2+} in the periodic table of the elements: Ca^{2+} shows coordinating properties similar to those of Mg^{2+}, but usually has a *lower* intrinsic affinity towards nucleic acids [35, 39]. It is interesting to note that mitochondria, in which the *cox1* gene carrying *Sc*.ai5γ resides, act as cellular Ca^{2+} stores, sequestering and releasing large amounts of Ca^{2+} depending on the metabolic needs of the cell [40, 41], thereby also being involved in controlled cell death [40, 42]. One could thus speculate whether a change in local metal ion concentration

within a cell (compartment) could be used by nature to regulate and/or switch the activity of a given ribozyme.

Materials and methods

Materials

T7 polymerase was prepared using standard procedures [43, 44]. Restriction enzymes for plasmid linearization were purchased from Roche Diagnostics and nucleoside 5′-triphosphates were purchased from Amersham Biosciences, now GE Healthcare (Otelfingen, Switzerland), except for UTP, which was obtained from Sigma-Aldrich (Buchs, Switzerland). $MgCl_2$ was utilized as a 1 M solution in H_2O in ultrapure quality from Fluka (Buchs, Switzerland). $CaCl_2$ solutions were prepared from ultrapure (better than 99.5%) $CaCl_2 \cdot 2H_2O$, also from Fluka.

DNA constructs and RNA transcription

The exD123 RNA (1,003 nucleotides in total, containing 293 nucleotides of the 5′-exon and domains 1, 2 and 3 from Sc.ai5γ) was transcribed from plasmid pJD3′-673 [45] linearized with HindIII. D5-58 (58 nucleotides in total, containing D5 flanked by 22 vector-derived nucleotides) was transcribed from plasmid pJDI5′-75 [45] linearized with HpaII. The shorter D5-36 construct [46] consisting of the 34 nucleotides of D5 plus one terminal G–C base pair to improve the transcription yield was transcribed from fully double stranded DNA templates provided by Microsynth (Balgach, Switzerland) [44]. Body-labeled exD123 RNA was transcribed with α-^{32}P-ATP (Amersham Biosciences) in volumes of 20 or 40 μL, purified by polyacrylamide gel electrophoresis (PAGE), and visualized by autoradiography with a Storm 860 phosphoimager (Amersham Biosciences) [38]. The labeled RNA was eluted by shaking the crushed gel pieces twice in 2 vol of 10 mM 3-(N-morpholino)propanesulfonic acid (MOPS), 1 mM EDTA, 250 mM NaCl, pH 6.5 for 2 h at 4 °C. The concentration was calculated via the specific activities from the scintillation counts obtained with a 22000CA liquid scintillation analyzer from Canberra Packard. Unlabeled D5-58 RNA was transcribed in a volume of 2 mL and purified by PAGE, electroeluted with a Biotrap system from Schleicher & Schuell (Dassel, Germany), and desalted with Centricon centrifugal filter devices (3000 MWCO) from Amicon. The concentrations of the nonradioactive RNA were determined with a Varian Cary 500 Scan UV–vis–near-IR spectrophotometer, using the extinction coefficient for D5-58 at 260 nm (ε_{260}) of 6.4×10^5 M^{-1} cm^{-1}. The samples were stored in 10 mM MOPS, pH 6.5, 1 μM EDTA at −20 °C.

Cleavage of exD123 by D5-58 at various Mg^{2+}-to-Ca^{2+} ratios

All trans-cleavage reactions were performed in RNase–DNase-free 0.5-mL reaction tubes in a total volume of 20 or 40 μL. The reactions were carried out in 40 mM MOPS (pH 7.5) and 500 mM KCl. RNA stock solutions were diluted individually and preincubated at 95 °C for 1 min to eliminate alternative RNA conformations [38]. The RNAs were left to cool separately to 45 °C. Only then were substrate (exD123) and catalyst (D5) mixed and the reaction was initiated by addition of premixed divalent metal ion stock solutions to a final total concentration of 100 mM. ^{32}P-exD123 was provided in a concentration of 1 nM and the concentration of D5 was varied from 0.05 to 6 μM.

Preliminary experiments were carried out for 30 min in the presence of 100 mM $MgCl_2$ or 100 mM $CaCl_2$ only, as well as different mixtures of $MgCl_2$ and $CaCl_2$ (80:20; 20:80; 50:50; 100:100; all numbers represent concentrations in millimoles per liter). The reaction in the presence of 100 mM $MgCl_2$ was performed with D5-58 as well as with the shorter hairpin D5-36 which has been used for the solution structure determination by NMR [46]. No difference between the two D5 constructs was detected. Later experiments were conducted with D5-58 to be able to compare the data directly with previously obtained results from trans-cleavage assays in the presence of Mg^{2+} alone [38].

To decipher the detailed kinetics of splicing in the presence of Ca^{2+}, trans-cleavage reactions were carried out in the presence of 0–5 mM Ca^{2+}, complemented with Mg^{2+} to a final divalent metal ion concentration of 100 mM. The following mixed-metal stock solutions were prepared prior to the reaction: 1 M $MgCl_2$, 990 mM $MgCl_2$/10 mM $CaCl_2$, 980 mM $MgCl_2$/20 mM $CaCl_2$, 960 mM $MgCl_2$/40 mM $CaCl_2$, and 950 mM $MgCl_2$/50 mM $CaCl_2$. These stock solutions were diluted 1:10 into the reaction mixture to initiate splicing. Two-microliter aliquots were taken at various times over the whole course of the reaction and immediately quenched with denaturing formamide loading buffer (82% formamide, 10 mM EDTA, and xyanole cyanide and bromphenol blue as dyes). The samples were kept on ice or frozen before being loaded onto a 5% polyacrylamide gel for analysis. After electrophoresis, the gels were dried on a Biometra Maxidry geldryer and visualized by autoradiography. The bands were analyzed by Image-Quant 5.2 (Amersham Biosciences).

Single-turnover kinetics

All experiments used for the kinetic analysis were performed using 1 nM ^{32}P-body-labeled exD123 as the

reaction substrate and an excess of 0.05–6 μM unlabeled "enzyme" D5. To ensure the presence of single-turnover conditions, an experiment with various subsaturating substrate concentrations (1–3 nM) was carried out. As expected for a reaction obeying pseudo-first-order kinetics, no variation in the reaction rate was observed. The reaction was monitored by the evolving product bands and the decrease in substrate bands. To minimize the effects of differential RNA degradation over time, the intensities of the bands were normalized by multiplication of the raw counts of the band with the ratio of the total counts of the three substrate and product bands per lane at $t = 0$ and the counts per lane at the time were analyzed. Furthermore, background counts unique to each lane were subtracted from the individual bands to account for random degradation. Because the large exD123 RNA undergoes random hydrolysis over time, only a time up to 80 min was taken into account. The observed rate constants (k_{obs}) for each time course were calculated from semilogarithmic plots of the fraction of the decrease in substrate/precursor, i.e., 1—increase of product versus time t, with m being the slope (Eq. 1):

$$\ln(\text{fp}) = mt + \ln 0.5 \left(\frac{m}{k_{obs}} + 1 \right). \tag{1}$$

Equation 1 was derived from the basic relationship between k_{obs} and the half-point of a reaction ($\tau_{1/2}$) obeying single-turnover conditions

$$k_{obs} = \frac{\ln 2}{\tau_{1/2}} \tag{2}$$

and the general formula

$$y = mx + a, \tag{3a}$$

where $y \equiv \ln(\text{fp})$ and $x \equiv t$. Thus, at the half-point of the reaction, Eq. 3a reads

$$\ln 0.5 = m\tau_{1/2} + a. \tag{3b}$$

Combination of Eqs. 2 and 3b gives

$$\tau_{1/2} = \frac{\ln 0.5 - a}{m} = \frac{\ln 2}{k_{obs}}. \tag{4}$$

Equation 4 is resolved for a and combined with Eq. 3a to give Eq. 1. Usually, $\tau_{1/2}$ is determined first via the slope in semilogarithmic plots of the fraction of precursor versus time and is subsequently used to calculate k_{obs} via Eq. 2. Equation 1 has the advantage that it links the experimental data directly to k_{obs}.

Final k_{obs} values for each condition were obtained by taking the weighted mean of the individual values with their error limits of at least two experiments. The relative standard error was used for the final k_{obs} values as it was generally larger than the absolute standard error. Although

variations in the observed rate constants were small for experiments from the same exD123 transcription performed within a few days, the kinetic parameters were found to vary up to 1.3-fold for experiments performed several weeks apart. This phenomenon has been observed before in studies of ribozyme kinetics using entirely different RNA stocks [38, 47, 48].

According to Michaelis–Menten kinetics, a plot of the observed reaction rates versus a range of D5 concentrations could be fitted to Eq. 5 describing a 1:1 bimolecular association curve, yielding k_{cat}, and K_D:

$$k_{obs} = k_{cat} \frac{([\text{exD123}] + [\text{D5}] + K_D) - \sqrt{([\text{exD123}] + [\text{D5}] + K_D)^2 - 4[\text{exD123}][\text{D5}]}}{2[\text{exD123}]}, \tag{5}$$

k_{obs} is the observed rate constant (per minute), k_{cat} is the maximum turnover rate (per minute), [exD123] and [D5] are the concentrations of the RNA constructs (millimoles per liter), and K_D is the dissociation constant for dissociation of D5 from exD123 [49–51].

trans-Cleavage reactions with other metal ions

The analogous trans-cleavage assay was performed in the presence of 90 mM Mg^{2+} and 10 mM Ca^{2+}, Mn^{2+}, Ni^{2+}, Zn^{2+}, Cd^{2+}, Pb^{2+}, or $[Co(NH_3)_6]^{3+}$ as described (vide supra). The substrate ^{32}P-exD123 was provided in a concentration of 1 nM and the enzyme D5 at 1 μM to reach single turnover reaction conditions [38]. Total aliquots of 3 or 6 μL were taken out either at 0, 30, and 90 min or at 0, 20, 40, and 90 or 105 min and the reaction was quenched by addition of an equal volume of formamide buffer dye. The content of these aliquots was analyzed on a 5% PAGE gel, run at 30–35 W for 4–5 h, dried and visualized by autoradiography. The bands were analyzed semiquantitatively by Image-Quant 5.2 (Amersham Biosciences).

Results

The first step of splicing at 100 mM Mg^{2+}

To investigate the effect of different metal ions on the first step of splicing of the group II intron Sc.ai5γ, a cleavage assay has to be applied that shows a uniform reaction and can be well characterized. For this purpose we used an established bipartite trans-splicing assay with the two RNA components exD123 and D5 [38, 52]. exD123 consists of 293 nucleotides of the 5′-exon covalently linked to D1 and domains 2 and 3 and acts as a reaction substrate (Fig. 1). D5 binds to D1, completing the catalytic core, and is unchanged during the reaction because a water molecule

acts as the nucleophile for the phosphodiester cleavage. The substrate concentration was kept constant at 1 nM, whereas D5, being the "enzyme," was added at increasing concentrations of 0.05, 0.1, 0.5, 1, 3, and 6 μM. Under these conditions, all substrate molecules are bound to the catalyst and the single-turnover reaction follows Michaelis–Menten kinetics.

In the presence of 100 mM MgCl$_2$ (and 0.5 M KCl), exD123 is almost entirely cleaved within 120 min into its 5′-exon and the intronic fragment D123 (Fig. 1). As observed previously [38], the intronic fragment is subsequently cleaved within D2, yielding secondary cleavage products of 560 and 150 nucleotides in length (Fig. 2). This secondary cleavage is much slower than splicing, and hence the splicing kinetics is not hampered. Combining the two secondary product bands with the D123 band, we find that the kinetic profile is interchangeable with the profile obtained from the 5′-exon evolution and the exact inverse of the disappearance of the substrate. These curves intersect at 50% of the reaction (Fig. 3).

The reaction rate k_{obs} for a given D5 concentration was calculated by fitting the experimental data in the linear range of the reaction with Eq. 1 (Fig. 3b, Table 1; see "Materials and methods"). As expected for Michaelis–Menten behavior, k_{obs} increases with higher D5 concentration, approaching a maximal turnover rate k_{cat}. To obtain k_{cat} and the apparent dissociation constant K_D of D5 binding to exD123, the k_{obs} values were plotted as a function of D5 concentration (Fig. 4a) and fitted with Eq. 5 (see "Materials and methods") reflecting 1:1 binding behavior [38, 49]. In the linear range of the reaction (Fig. 3b), exD123 is saturated with D5, i.e., single-turnover conditions are present and product release is not an issue. It is known that no rate-limiting conformational change occurs in the enzyme–substrate complex [24, 25], and k_{cat} therefore reflects neither binding nor product release but is considered equal to the rate of the chemical step k_{chem}. The values we obtained—$k_{cat} = 0.045 \pm 0.002$ min^{-1} and $K_D = 169 \pm 30$ nM (100 mM Mg^{2+}, pH 7.5)—are in good agreement with previously reported results ($k_{cat} = 0.041 \pm 0.001$ min^{-1}, $K_D = 270 \pm 25$ nM [38]).

Metal ions other than Mg^{2+} inhibit the trans-cleavage reaction

Metal ions other than Mg^{2+} are known to either inhibit or accelerate the reactions catalyzed by different ribozymes. Here, we chose to investigate the effect of a variety of metal ions that are commonly used in biochemistry and structural biology, i.e., Mn^{2+}, Ni^{2+}, Zn^{2+}, Cd^{2+}, Pb^{2+}, and [Co(NH$_3$)$_6$]$^{3+}$, on the first step of splicing of *Sc*.ai5γ (Fig. 5). In the presence of 90 mM Mg^{2+} and 10 mM concentration of each divalent metal ion (at a background

of 0.5 M KCl), the same trans-splicing reaction as described in the previous section was carried out and compared with the Mg^{2+}-only reaction. Hence, all M^{2+} conditions had the same ionic strength ($I = 0.8$), except for the case of [Co(NH$_3$)$_6$]$^{3+}$, where $I = 0.83$ and thus is slightly higher. All reactions were repeated at least three times and aliquots of the reaction mixture were quenched with formamide buffer at either 0, 30, and 90 min or 0, 20, 40, and 90 or 105 min. PAGE analysis revealed the familiar band pattern (Fig. 2) with decreasing intensities of the substrate exD123 and concomitantly increasing intensities of four product bands (Fig. 5).

As can be seen in Fig. 6, Mn^{2+} has the least influence on the trans-splicing reaction: After 40 min, 82% of the substrate exD123 has been cleaved, compared with 88% in the presence of Mg^{2+} only. Ca^{2+} and Cd^{2+} both exhibit a comparable effect, with about 70% of substrate being cleaved. trans-Splicing in the presence of 10 mM [Co(NH$_3$)$_6$]$^{3+}$ also works quite well, as still 64% cleavage occurs within 40 min. In all of these cases, no enhanced unspecific cleavage of the RNA could be detected (Fig. 5). This is different for Ni^{2+}, Zn^{2+}, and Pb^{2+}, which all show a strong inhibitory effect. For example, in the case of Ni^{2+}, an 80% decrease in the intensity of the substrate band over the course of the reaction is observed, but no simultaneous increase in the product D123 was detected at any time
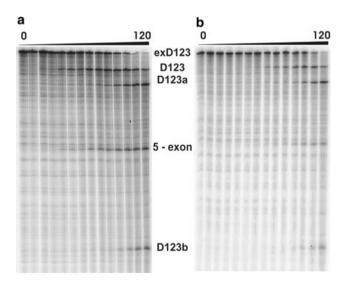

Fig. 2 Gels of the time course (up to 120 min, see also Fig. 3) of two trans-cleavage assays with 1 nM exD123 and 0.1 μM D5. **a** Reaction in the presence of 100 mM Mg^{2+} only, giving an observed rate constant $k_{obs} = 0.016 \pm 0.001$ min^{-1}. **b** Reaction in the presence of 5 mM Ca^{2+} and 95 mM Mg^{2+} ($k_{obs} = 0.008 \pm 0.001$ min^{-1}). In addition to the decreasing substrate band (exD123) and the increasing intensity of the primary products D123 and 5′-exon, also the two secondary cleavage bands (D123a and D123b) with lengths of 560 and 150 nucleotides can be seen. As D123a and D123b evolve only after the first splicing event, they do not interfere with the rate of the first step of splicing
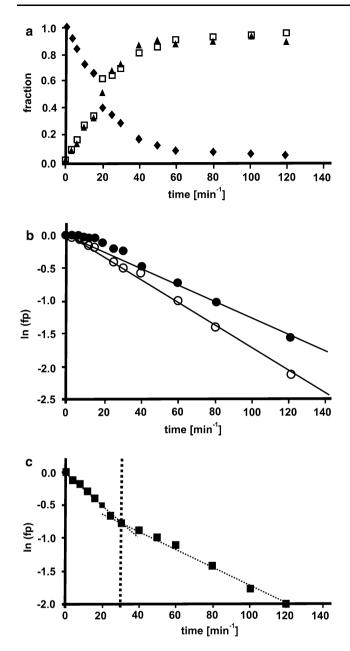
Fig. 3 Calculation of the observed rate constants k_{obs} for the cleavage of 1 nM exD123 by 1 μM D5 in the presence of Mg^{2+} and Ca^{2+}. **a** Time course for the cleavage of exD123 (*diamonds*) into D123 (*squares*) and 5′-exon (*triangles*) in the presence of 99 mM $MgCl_2$ and 1 mM $CaCl_2$. The plots intersect at 50% of the reaction at $\tau_{1/2} = 20$ min. **b** ln (fp) (with fp being the fraction of precursor) versus time for the splicing reaction in the presence of 100 mM $MgCl_2$ (*open circles*) as well as 99 mM $MgCl_2$ and 1 mM $CaCl_2$ (*filled circles*). Ca^{2+} clearly lowers the observed reaction rate k_{obs}. k_{obs} was calculated from the linear regression according to Eq. 1. **c** Active replacement of Mg^{2+} by Ca^{2+}. The splicing reaction is initiated with 95 mM Mg^{2+} only. Addition of 5 mM Ca^{2+} after 30 min results in an immediate loss of the observed rate as is evident from the kink in the data profile. k_{obs} values before and after the addition of Ca^{2+} are comparable to the ones observed when the full time course was carried out in the presence of 95 mM Mg^{2+}/5 mM Ca^{2+} or 100 mM Mg^{2+} only, respectively (Table 2)

(Fig. 5). Hence, the decrease in substrate is solely due to unspecific degradation. A similar observation is made with Zn^{2+}, whose presence leads to the complete degradation of the substrate exD123 within the first 30 min. Again, no specific cleavage, i.e., splicing, was detected at any time in the course of the reaction. The addition of 10 mM Pb^{2+} also does not result in any specific splicing, but again leads to complete unspecific degradation of the substrate. In addition, a white precipitate could be observed after 10 min of incubation consisting most likely of lead–hydroxo species. Both Zn^{2+} and Pb^{2+} are well known to promote phosphate–diester hydrolysis. These two examples illustrate that the ability of a metal ion to activate a nucleophile and accelerate cleavage is not the sole requirement in group II intron splicing.

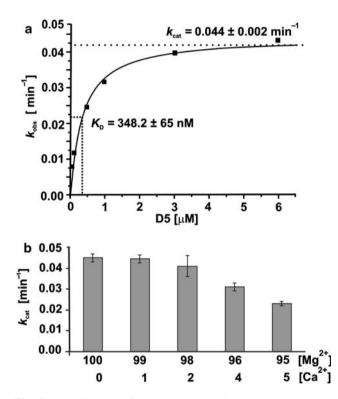### Ca^{2+} actively inhibits the *trans*-splicing reaction

In subsequent experiments we concentrated on the effect of Ca^{2+} on the splicing reaction, as this divalent metal ion occurs also freely in the cell, though tightly regulated. Experiments analogous to those described in the previous section were carried out in presence of various amounts of $CaCl_2$. Using 1 nM exD123 and 3 μM D5, we detected no product formation in either 100 mM $CaCl_2$ alone or 1:1 mixtures of $MgCl_2$ and $CaCl_2$ at either 50 or 100 mM concentration each (data not shown). Ribozyme constructs of *Sc*.ai5γ are known to be correctly folded and active in vitro at 50 mM Mg^{2+} alone [53]. Hence, these results already illustrate that Ca^{2+} cannot substitute Mg^{2+} in order to reach the active fold. Furthermore, Ca^{2+} obviously interferes with Mg^{2+} binding either during folding or in the active complex, thereby completely inhibiting the first step of splicing under these conditions.

To gain further information on the competition between Mg^{2+} and Ca^{2+} binding and the effect on splicing of the group II intron *Sc*.ai5γ, we performed a series of *trans*-cleavage assays at lower Ca^{2+} concentrations, i.e., 1–5 mM $CaCl_2$. The ionic strength of the reaction mixtures was kept constant by complementing 100 mM M^{2+} with $MgCl_2$. In this way, the kinetic profiles of the reactions with different Ca^{2+} concentrations can be directly compared with each other. Under all Ca^{2+} concentrations applied (1–5 mM), the splicing reaction still obey pseudo-first-order kinetics up to at least 60 min. At later times, deviation from linearity is observed because random hydrolysis becomes significant as has also previously been described with Mg^{2+} only [38]. Using the data points in the linear range of each experiment, we calculated the observed rates k_{obs} and $\tau_{1/2}$, the half-time of the reaction (Eqs. 1, 2, Fig. 3b). Irrespective of the Mg^{2+}-to-Ca^{2+} ratio applied, the reaction becomes faster with increasing D5

Table 1 Observed first-order rate constants k_{obs}, reaction half-times $\tau_{1/2}$, and maximal turnover rates k_{cat} for the *trans*-cleavage experiments of 1 nM exD123 with 0.1 μM D5 for the Mg^{2+}-to-Ca^{2+} ratios indicated. The dissociation constants K_D for D5 binding to exD123 for each Mg^{2+}-to-Ca^{2+} ratio are given in the last column

Mg^{2+}-to-Ca^{2+} ratio (mM)	k_{obs} (min^{-1})	$\tau_{1/2}$ (min)	k_{cat} (min^{-1})	K_D
100:0	0.016 ± 0.001	43.3 ± 2.7	0.045 ± 0.002	168.7 ± 29.7
99:1	0.012 ± 0.001	57.8 ± 4.8	0.044 ± 0.002	348.2 ± 65.0
98:2	0.013 ± 0.001	53.3 ± 4.1	0.041 ± 0.005	291.1 ± 162.0
96:4	0.011 ± 0.002	63.0 ± 11.4	0.031 ± 0.002	122.2 ± 44.4
95:5	0.008 ± 0.001	86.6 ± 10.8	0.023 ± 0.001	154.2 ± 43.6

Fig. 4 Determination of k_{cat} and K_D. **a** k_{obs} values versus D5 concentration fitted to a 1:1 bimolecular association curve (Eq. 5). For the experiment shown (99 mM MgCl$_2$ and 1 mM CaCl$_2$), the maximal turnover rate at D5 saturation $k_{cat} = 0.044 \pm 0.002$ min^{-1} and a dissociation constant of D5 towards exD123 $K_D = 348.2 \pm 65$ nM were obtained. **b** Decrease of k_{cat} with increasing concentrations of Ca^{2+} in the reaction mixture. A concentration of only 5 mM Ca^{2+} in excess of 95 mM Mg^{2+} slows the rate of the *trans*-cleavage reaction down to about one half

concentrations as is expected for a Michaelis–Menten behavior. The experimental data obtained for the different Mg^{2+}-to-Ca^{2+} ratios were evaluated analogously to those for the Mg^{2+}-only case described in the previous section, yielding k_{cat} and K_D values (Fig. 4). The dissociation constants K_D for D5 binding to exD123 vary between 120 and 560 nM, which is in a range of values published before for the Mg^{2+}-only case [38, 52]. No obvious dependence of K_D versus Ca^{2+} concentration (Table 1) was observed,

indicating that the presence of Ca^{2+} does not directly interfere with the binding of D5 to D1.
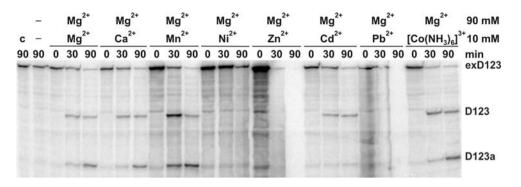
In contrast, the maximum turnover rate k_{cat} exhibits a strong dependence on the Ca^{2+} concentration. This rate decreases steadily with increasing amounts of Ca^{2+} (Fig. 4b, Table 1). For example in the presence of only 5 mM Ca^{2+} (and 95 mM Mg^{2+}), k_{cat} is reduced to about 50% ($k_{cat} = 0.023 \pm 0.01$ min^{-1}) compared with the situation in 100 mM Mg^{2+} ($k_{cat} = 0.045 \pm 0.02$ min^{-1}). Upon further increase of the Ca^{2+} concentration, k_{cat} further decreases and in the presence of 10 mM Ca^{2+} no splicing product can be detected anymore up to 20 min. This finding shows that at least one high-affinity binding site for Ca^{2+} must be present within the three-dimensional architecture of the exD123-D5 complex that interferes directly with catalysis.
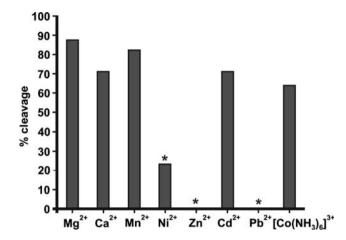
Ca^{2+} inhibits the early steps of folding

The *trans*-splicing assays in the presence of Ca^{2+} reveal one further interesting fact. At the beginning of the *trans*-splicing reaction, product formation was retarded considerably, i.e., none was observed for the first 10 min (Fig. 3b). Such a delayed start of the reaction has also been observed by us and others [38, 54, 55] if only Mg^{2+} is present, although not to such a large extent. This initial phase of slower kinetics is indicative of the folding of D1 and/or docking of domains 2 and 3 and D5 to this scaffold. All these processes are induced by the addition of divalent metal ions and take place prior to the splicing reaction. The initial collapse of D1 is the rate-limiting step of the folding pathway, with $k_{fold} \approx 1$ min^{-1} [56]. The slow start of the cleavage reaction can be prevented by preincubation of the individual components with Mg^{2+} (or a corresponding Mg^{2+}/Ca^{2+} mixture, respectively) for 10 min at 45 °C (data not shown). The reaction rates k_{obs} calculated from the linear phases of the experiments with and without preincubation are the same within the error limits for all Mg^{2+}-to-Ca^{2+} ratios applied. As a side effect, preincubation with divalent metal ions at 45 °C strongly accelerates random degradation of the RNA to an

Fig. 5 *trans*-Cleavage assays in the presence of 90% Mg^{2+} and 10 mM of another metal ion. Shown are the cleavage patterns at reaction times of 0, 30, and 90 min each. The control lane (*c*) contains only exD123 and lane 2 exD123, 500 mM KCl, and 40 mM MOPS (pH 7.2), but no divalent metal ions

Fig. 6 Percentage of exD123 spliced after 40 min of the *trans*-cleavage reaction in the presence of 90 mM Mg^{2+} and 10 mM Ca^{2+}, Mn^{2+}, Ni^{2+}, Zn^{2+}, Cd^{2+}, Pb^{2+}, or $[Co(NH_3)_6]^{3+}$. In the case of Ni^{2+}, Zn^{2+}, and Pb^{2+}, exD123 degrades without the appearance of product bands at any time (marked with an *asterisk*), i.e., these three metal ions completely inhibit splicing

extent that only a time span up to 40 min could be used for the kinetic analysis. For this reason we did not routinely preincubate the individual components before the reaction.

The extended time that exD123 and D5 need to assemble to the active species in the presence of small amounts of Ca^{2+} strongly indicates that Ca^{2+} also interferes with the folding pathway. Considering that the K_D values for D5 binding to exD123 show no dependence on Ca^{2+} concentration, it seems likely that the interference of Ca^{2+} occurs earlier, i.e., during the collapse of D1.

Ca^{2+} competes actively with Mg^{2+} for its binding site

In the previous sections we have shown that Ca^{2+} interferes with both catalysis and folding, when added simultaneously with Mg^{2+} to the reaction mixture containing exD123 and D5. Obviously, in such an experimental setup, both alkaline earth metal ions have a priori the same chance to bind to any metal ion binding site within the active three-dimensional exD123/D5 complex. Mg^{2+} is always present in excess,

which means that Ca^{2+} must bind more strongly to at least one certain site. It is an open question whether Ca^{2+} binds to a site(s) unoccupied by Mg^{2+} or replaces Mg^{2+}, or both. However, in order to both slow down folding and inhibit catalysis, it is most likely that several Ca^{2+} ions are involved in the process.

To examine whether the inhibiting Ca^{2+} ion(s) needs to be incorporated during the folding process, or if Ca^{2+} can actively displace Mg^{2+} from the crucial binding site(s) once the ribozyme has folded, we performed an "on-pathway" inhibition experiment. The splicing reaction was initiated in the presence of 95 mM Mg^{2+} only. At a specific time (12 or 30 min after the start), 5 mM $CaCl_2$ was added to the reaction mixture. Plotting product formation versus time reveals a sharp kink at the time when 5 mM Ca^{2+} was added to the reaction mixture (Fig. 3c). Separate analysis of the data before and after Ca^{2+} addition yielded two different k_{obs} values. At a concentration of 0.1 μM D5 and addition of Ca^{2+} 30 min after the start of the reaction, $k_{obs/30a} = 0.19$ min^{-1} (before addition of Ca^{2+}) and $k_{obs/30b} = 0.007$ min^{-1} (after addition of Ca^{2+}) were obtained (Table 2). Both values agree surprisingly well within their error limits with the respective k_{obs} values determined in the presence of Mg^{2+} only and a 95:5 mixture of the two divalent metal ions (0.16 and 0.008 min^{-1}, respectively). Similar values were obtained from experiments where Ca^{2+} was added after 12 min (Table 2). This result clearly shows that Ca^{2+} is able to actively displace Mg^{2+} from its binding site even within the core of the folded ribozyme.

Discussion

Mg^{2+} is an essential cofactor for the large group II intron ribozymes, being necessary for folding into the active tertiary structure as well as for catalysis [21, 53, 56–59]. Although the effect of metal ions on catalytic RNA has been studied extensively with ribozymes other than group II introns [5, 9, 29, 35, 60–66], it is still not known in detail how divalent metals influence the catalytic efficiency of these molecular machines.

Table 2 Observed rates k_{obs} for the *trans*-cleavage reaction with 1 nM exD123 and a series of D5 concentrations carried out in 95 mM Mg^{2+} with 5 mM Ca^{2+} added after 12 and 30 min, respectively. The plot of ln (fp) versus time shows a sharp kink at the time of Ca^{2+} addition (Fig. 3c). Before Ca^{2+} addition ($k_{obs/12a}$ and $k_{obs/30a}$), the observed rate constants k_{obs} are comparable to the ones measured in 100 mM Mg^{2+} $k_{obs/100}$ (columns 2–4). After Ca^{2+} addition ($k_{obs/12b}$ and $k_{obs/30b}$), the reaction slows down to rates close to the ones measured for the *trans*-cleavage assays in 95 mM Mg^{2+} and 5 mM Ca^{2+}, i.e., $k_{obs/95}$ (columns 5–7). D5 concentrations are given in micromoles per liter and the rates in per minute, with errors corresponding to at least one standard deviation

D5	$k_{obs/100}$	$k_{obs/12a}$	$k_{obs/30a}$	$k_{obs/95}$	$k_{obs/12b}$	$k_{obs/30b}$
0.05	0.012 ± 0.001	$-^a$	0.012 ± 0.001	0.007 ± 0.001	0.008 ± 0.001	0.006 ± 0.001
0.10	0.016 ± 0.001	0.013 ± 0.001	0.019 ± 0.001	0.008 ± 0.001	0.008 ± 0.001	0.007 ± 0.001
1.00	0.037 ± 0.005	0.041 ± 0.002	0.041 ± 0.001	0.022 ± 0.001	0.033 ± 0.001	$-^a$

^{a} These rates could not be determined with good enough accuracy because of either too slow a reaction ($k_{obs/12a}$) or not enough time in the linear phase of the splicing reaction ($k_{obs/30b}$)

Here we studied the effect of various metal ions on group II intron splicing, choosing *Sc*.ai5γ as one of the best characterized ribozymes of this class. We thereby focused on the effect of Ca^{2+} because *Sc*.ai5γ resides in the mitochondria, one of the cell's main Ca^{2+} storage sites. Ca^{2+} is a physiologically very important metal ion, e.g., playing roles in homeostasis of the cell in general, in Ca^{2+} signaling [67, 68], enzyme activation [69], and energy production [70]. Thus, concentrations of Ca^{2+} in living cells are strictly regulated. Mitochondria sequester and release Ca^{2+} with high efficiency [67, 68, 71–74]. Apart from its role in Ca^{2+} homeostasis, mitochondrial Ca^{2+} also seems to be important in cell apoptosis: overexpression of antiapoptotic Bcl-2, which is preferentially located in mitochondria, leads to a greatly increased Ca^{2+} uptake capacity of such cells [42, 67, 75]. Furthermore, release of cytochrome *c* from the mitochondrial intermembrane compartment is thought to activate caspases and eventually lead to apoptosis of the cell [76]. Although the role of cytochrome *c* in apoptosis is thought to be independent of its respiratory function, it is striking that *Sc*.ai5γ, whose self-splicing activity can be impaired by Ca^{2+} in vitro, resides in the yeast cytochrome *c* oxidase gene I [77], suggesting a potential role in apoptosis in vivo.

Our mixed metal ion studies reveal an inhibitory effect of Ca^{2+} on self-splicing already at a concentration of 1 mM on a 99 mM Mg^{2+} background. At a Ca^{2+} concentration of 5 mM, the turnover rate k_{cat} is reduced by one half from 0.045 ± 0.02 min^{-1} at 100 mM Mg^{2+} to 0.023 ± 0.01 min^{-1} (Table 1). A reduction in cleavage rate solely due to the lower concentration of Mg^{2+} can be excluded for the following reason: upon addition of Mg^{2+}, *Sc*.ai5γ folds directly to the active state with a midpoint of 40–50 mM Mg^{2+} [25]. Hence, above 90 mM Mg^{2+} a change in concentration should only have very small effects. Indeed, the rates measured at 100 and 95 mM Mg^{2+} correspond to each other within error limits of three standard deviations (Table 2).

Intriguingly, even if Ca^{2+} is added to the reaction mixture at a later time, this metal ion clearly inhibits product formation as is evident by the sharp kink in the semilogarithmic plot of the decrease of the precursor fraction versus time (Fig. 3). All these results are a clear indication that Ca^{2+} is able to actively replace Mg^{2+} from at least one of its binding sites and consequently inhibit splicing. Evidently such an exchange of the two alkaline earth ions can only take place if the affinity of Ca^{2+} to the binding site is higher than that of the naturally applied Mg^{2+}. The amount of increased Ca^{2+} affinity at this site can be estimated: a 50% reduction in the catalytic rate k_{cat} is achieved in the presence of a 20-fold excess of Mg^{2+} over Ca^{2+}. Assuming that the binding of Ca^{2+} at a specific site leads to a total (i.e., 99%) loss in activity, its affinity must be about 2,000 times higher than that for Mg^{2+} at the site of displacement.

How do these findings compare with the ligand binding properties and known affinity constants of these two metal ions to nucleotides? Both alkaline earth metal ions prefer oxygen donor ligands over the softer nitrogen, but being below Mg^{2+} in the periodic table, Ca^{2+} has an ionic radius which is about 40% larger (100 pm, compared with 72 pm; Table 3) [78, 79]. Consequently, the cation-to-ligand distance is also longer (237 vs. 204 pm) [80]. Owing to the difference in size also the coordination numbers differ slightly: whereas Mg^{2+} is generally octahedral, Ca^{2+} often binds eight donor atoms [79]. On the basis of these different coordinating properties, it is expected that Ca^{2+} forms weaker complexes. Indeed, the measured stability constants for the M(AMP) complexes (AMP^{2-} is adenosine 5′-monophosphate) $\log K_{Mg(AMP)}^{Mg} = 1.60 \pm 0.02$ and $\log K_{Ca(AMP)}^{Ca} = 1.46 \pm 0.02$ [81] or the M(ATP)$^{2-}$ complexes (ATP^{4-} is adenosine 5′-triphosphate) $\log K_{Mg(ATP)}^{Mg} = 4.29 \pm 0.03$ and $\log K_{Ca(ATP)}^{Ca} = 3.91 \pm 0.03$ [82] illustrate the different coordinating strengths. Similar differences are found for related nucleotides and derivatives thereof [39, 83, 84].

Table 3 Comparison of some physicochemical properties of Mg^{2+}, Ca^{2+}, Mn^{2+}, Ni^{2+}, Zn^{2+}, Cd^{2+}, and Pb^{2+} in aqueous solution. Given are the ionic radii [78] and the preferred coordination number (CN) of the M^{2+} ions, the enthalpy of hydration (ΔH_{hydr}) [80], the distance between the metal ion and a coordinated water molecule [80, 94], the acidity constant $pK^H_{M(H_2O)_6}$ of a water molecule in the hexa-aqua complex [95], as well as the ligand-exchange rate from the first coordination sphere of the metal ion (k_{exch}) [96–99]

	Mg^{2+}	Ca^{2+}	Mn^{2+}	Ni^{2+}	Zn^{2+}	Cd^{2+}	Pb^{2+}
Ionic radius (pm)	72	100 (112)[a]	83[b]	69	74[c]	95	119
CN	6	6 (8)[a]	6	6	4	6	–[d]
Preferred ligands	O	O	O/N	N/O	N/O	N/O	O
ΔH_{hydr} (kJ mol^{-1})	1858	1570 (1,657)[a]	1762	1950	1871	1640	1431
M$\cdots$OH$_2$ (Å)	2.04	2.37 (2.48)[a]	2.18	2.12	2.15	2.35	2.60
$pK^H_{M(H_2O)_6}$ (25 °C)	11.44	12.85	10.59	9.86	8.96[e]	10.2	7.8
k_{exch} (s^{-1})	6.7×10^5	$\approx 10^9$	2.1×10^7	3.2×10^4	4.1×10^8	6.8×10^8	1.0×10^{10}

[a] The numbers in *parentheses* refer to CN = 8

[b] High-spin electron configuration

[c] For CN = 6

[d] Pb^{2+} has no really preferred coordination number. It can be 4, 6, 7, 8, or 9. The value given refers to CN = 6 [79]

[e] With other liganding sites present in the coordination sphere of Zn^{2+}, the pK_a value for hydrolysis is shifted towards the neutral pH range [100]

The ligand-exchange rate of Ca^{2+} is about 1,000-fold faster than that of Mg^{2+} (10^9 vs. 10^6 s^{-1}; Table 3), suggesting that Ca^{2+} binds faster to the RNA during the folding process and later on is removed by Mg^{2+} owing to the difference in binding affinity. If such a mechanism of inhibition takes place, one should observe only an initial decline in rate. Indeed, the initial folding process upon addition of Mg^{2+} ions is inhibited by Ca^{2+}, as, e.g., in the presence of 1% Ca^{2+} product formation can only be detected after 10 min (Fig. 3b). However, as soon as all Ca^{2+} ions have been replaced by Mg^{2+}, the full rate of splicing should be reconstituted. In contrast, we find that Ca^{2+} inhibits the splicing reaction itself even in a large excess of Mg^{2+}. This suggests the presence of at least one crucial binding pocket that is "optimized" for Ca^{2+}, possibly by being too large for Mg^{2+} and by offering more donor sites for Ca^{2+}. The presence of a specific binding site for Ca^{2+} is corroborated by the observation that addition of Ca^{2+} to the ongoing splicing reaction of the folded ribozyme slows down the reaction immediately. A specificity for Ca^{2+} over Mg^{2+} is already known from low molecular weight complexes as well as certain proteins: e.g., the ligand Bistris forms an approximately 80 times more stable complex with Ca^{2+} than with Mg^{2+} ($\log K^{Mg}_{Mg(Bistris)} = 0.34 \pm 0.05$ and $\log K^{Ca}_{Ca(Bistris)} = 2.25 \pm 0.02$) [85] and certain sites in the protein calbindin D_{9k} do not bind Mg^{2+} even in absence of Ca^{2+} [86].

At this point one may speculate what the local effect of Ca^{2+} in the group II intron *Sc*.ai5γ might be: the replacement of Mg^{2+} by Ca^{2+} at a specific site may lead to a local geometrical change and thus interrupt a crucial tertiary interaction, or even alter the catalytic core itself.

Considering the fast and large changes in Ca^{2+} concentration within mitochondria, a possible effect on splicing of *Sc*.ai5γ in vivo is an interesting possibility.

Similarly to Ca^{2+} also other divalent metal ions lead to an inhibition of the splicing reaction (Fig. 6). Mn^{2+} seems to be the best substitute for Mg^{2+} in group II introns, as the *trans*-cleavage reaction is hardly inhibited. Mn^{2+} is slightly larger than Mg^{2+} (83 vs. 72 pm; Table 3) but has the same preference for an octahedral coordination sphere [78, 79]. According to the Irving–Williams series [87] its complexes are in general slightly more stable than those of Mg^{2+}. The hammerhead ribozyme [10], the *Tetrahymena* ribozyme [88], and ribonuclease P [89] have been shown to be active or sometimes even accelerated in the presence of Mn^{2+}. It is therefore no surprise that a certain portion of the Mg^{2+} needed for the splicing reaction of *Sc*.ai5γ can be replaced by Mn^{2+}.

It is interesting to note that exD123 is spliced in the presence of $[Co(NH_3)_6]^{3+}$, albeit more slowly than with Mg^{2+} alone. Because of its inert NH_3 ligands, $[Co(NH_3)_6]^{3+}$ may replace Mg^{2+} without much distortion of the local RNA structure only at binding sites which require an exclusively outer-sphere coordination mode of Mg^{2+}. At sufficiently high concentrations of Mg^{2+}, $[Co(NH_3)_6]^{3+}$ will thus coordinate only to outer-sphere binding sites, whereas partly inner-sphere binding sites can still be occupied by $[Mg(H_2O)_m]^{n+}$.

Interestingly, Cd^{2+}, having an ionic radius comparable in size to that of Ca^{2+}, slows down the splicing reaction to about the same extent. However, Cd^{2+} has a much higher affinity towards nitrogen ligands than Ca^{2+} and is expected to replace Mg^{2+} only very selectively, i.e., only if inner-sphere coordination to a N7 position of a purine nucleobase

residue can take place [35]. These results therefore underline the notion that besides a reasonably high affinity of a given metal ion also its individual coordinating properties as well as the accessibility of certain binding sites play an important role in the specific metal ion binding within group II introns.

The remaining metal ions examined exhibit a different effect (Fig. 6): Zn^{2+} and Pb^{2+} lead to a fast nonspecific degradation of the substrate (Fig. 5). Indeed, both metal ions have a high affinity for phosphate residues and a significant tendency to form hydroxo complexes. Thus, they are ideal cations to activate water for nucleophilic attacks in the physiological pH range and Zn^{2+} is for such a purpose also found in nucleases [90, 91]. Hence, the observed nonspecific degradation effects are not too surprising. Ni^{2+} fits into the same picture, having a comparable phosphate affinity but in addition a more pronounced affinity towards nitrogen sites and a smaller tendency to form hydroxo complexes [92]. Indeed, also in the presence of Ni^{2+} a nonspecific cleavage is observed but with a lower effectiveness than Zn^{2+} and Pb^{2+} (Fig. 5).

In the cases of the P4–P6 domain of the *Tetrahymena* group I intron [93] and the hammerhead ribozyme [9], it has been shown that the effect of different metal ions on folding and catalysis, respectively, follows to a large extent the Irving–Williams series. In the case of *Sc*.ai5γ, no such trend following the Irving–Williams series [87] or the *stability ruler* of Martin [79] can be observed. It thus appears that in group II introns, or most likely in large RNAs in general, specific binding pockets exist, which bind metal ions other than Mg^{2+} much more tightly and more selectively. Whether such a selectivity and specificity has evolved on purpose, i.e., providing the organism with a means to fine-tune the reactivity of a given naturally occurring ribozyme, or if the resulting acceleration or inhibition happens by chance remains to be seen.

References

1. Gesteland RF, Cech TR, Atkins JF (2006) The RNA world. Cold Spring Harbor Press, New York
2. Joyce GF (1993) Pure Appl Chem 65:1205–1212
3. Beaudry AA, Joyce GF (1992) Science 257:635–641
4. Kazakov S, Altman S (1992) Proc Natl Acad Sci USA 89:7939–7943
5. Sigel RKO, Pyle AM (2007) Chem Rev 107:97–113
6. O'Rear JL, Wang S, Feig AL, Beigelman L, Uhlenbeck OC, Herschlag D (2001) RNA 7:537–545
7. Murray JB, Seyhan AA, Walter NG, Burke JM, Scott WG (1998) Chem Biol 5:587–595
8. Curtis EA, Bartel DP (2001) RNA 7:546–552
9. Roychowdhury-Saha M, Burke DH (2006) RNA 12:1846–1852
10. Dahm SC, Uhlenbeck OC (1991) Biochemistry 30:9464–9469
11. Chowrira BM, Berzal-Herranz A, Burke JM (1993) Biochemistry 32:1088–1095
12. Li J, Lu Y (2000) J Am Chem Soc 122:10466–10467
13. Santoro SW, Joyce GF (1997) Proc Natl Acad Sci USA 94:4262–4266
14. Faulhammer D, Famulok M (1997) J Mol Biol 269:188–202
15. Faulhammer D, Famulok M (1996) Angew Chem Int Ed 35:2837–2841
16. Li J, Zheng WC, Kwon AH, Lu Y (2000) Nucleic Acids Res 28:481–488
17. Lehman N, Joyce GF (1993) Nature 361:182–185
18. Lehman N, Joyce GF (1993) Curr Biol 3:723–734
19. Burton AS, Lehman N (2006) Biochimie 88:819–825
20. Costa M, Fontaine JM, Goër SL, Michel F (1997) J Mol Biol 274:353–364
21. Pyle AM (2002) J Biol Inorg Chem 7:679–690
22. Sigel RKO (2005) Eur J Inorg Chem 12:2281–2292
23. Waldsich C, Pyle AM (2008) J Mol Biol 375:572–580
24. Waldsich C, Pyle AM (2007) Nat Struct Mol Biol 14:37–44
25. Fedorova O, Zingler N (2007) Biol Chem 388:665–678
26. Gordon PM, Piccirilli JA (2001) Nat Struct Biol 8:893–898
27. Toor N, Keating KS, Taylor SD, Pyle AM (2008) Science 320:77–82
28. Hertweck M, Müller MW (2001) Eur J Biochem 268:4610–4620
29. Sigel RKO, Pyle AM (2003) Met Ions Biol Syst 40:477–512
30. Sigel RKO, Vaidya A, Pyle AM (2000) Nat Struct Biol 7:1111–1116
31. Boudvillain M, de Lencastre A, Pyle AM (2000) Nature 406:315–318
32. Boudvillain M, Pyle AM (1998) EMBO J 17:7091–7104
33. Fedorova O, Pyle AM (2005) EMBO J 24:3906–3916
34. Gordon PM, Fong R, Piccirilli JA (2007) Chem Biol 14:607–612
35. Freisinger E, Sigel RKO (2007) Coord Chem Rev 251:1834–1851
36. Furler M, Knobloch B, Sigel RKO (2008) Inorg Chim Acta. doi:10.1016/j.ica.2008.1003.1095
37. Fedorova O, Su LJ, Pyle AM (2002) Methods 28:323–335
38. Pyle AM, Green JB (1994) Biochemistry 33:2716–2725
39. Sigel RKO, Song B, Sigel H (1997) J Am Chem Soc 119:744–755
40. Babcock DF, Hille B (1998) Curr Opin Neurobiol 8:398–404
41. Carafoli E (1979) FEBS Lett 104:1–5
42. Zamzami N, Hirsch T, Dallaporta B, Petit PX, Kroemer G (1997) J Bioenerg Biomembr 29:185–193
43. Davanloo P, Rosenberg AH, Dunn JJ, Studier FW (1984) Proc Natl Acad Sci USA A81:2035–2039
44. Gallo S, Furler M, Sigel RKO (2005) Chimia 59:812–816
45. Jarrell KA, Dietrich RC, Perlman PS (1988) Mol Cell Biol 8:2361–2366
46. Sigel RKO, Sashital DG, Abramovitz DL, Palmer AG III, Butcher SE, Pyle AM (2004) Nat Struct Mol Biol 11:187–192
47. Herschlag D, Cech TR (1990) Biochemistry 29:10172–10180
48. Fedor MJ, Uhlenbeck OC (1992) Biochemistry 31:12042–12054
49. Sigel RKO, Freisinger E, Lippert B (2000) J Biol Inorg Chem 5:287–299
50. Erat MC, Sigel RKO (2007) Inorg Chem 46:11224–11234
51. Mikkola S, Stenman E, Nurmi K, Yousefi-Salakdeh E, Stromberg R, Lonnberg H (1999) J Chem Soc Perkin Trans 2 1619–1625
52. Chin K, Pyle AM (1995) RNA 1:391–406

53. Swisher JF, Su LJ, Brenowitz M, Anderson VE, Pyle AM (2002) J Mol Biol 315:297–310
54. Chu VT, Liu Q, Podar M, Perlman PS, Pyle AM (1998) RNA 4:1186–1202
55. Costa M, Michel F (1995) EMBO J 14:1276–1285
56. Su LHJ, Brenowitz M, Pyle AM (2003) J Mol Biol 334:639–652
57. Qin PZ, Pyle AM (1997) Biochemistry 36:4718–4730
58. Pyle AM (1996) In: Eckstein F, Lilley DMJ (eds) Nucleic acids and molecular biology. Springer, New York, pp 75–107
59. Pyle AM (1996) Met Ions Biol Syst 32:479–519
60. Flynn-Charlebois A, Lee N, Suga H (2001) Biochemistry 40:13623–13632
61. Butcher SE (2001) Curr Opin Struct Biol 11:315–320
62. Doherty EA, Doudna JA (2001) Annu Rev Biophys Biomol Struct 30:457–475
63. Fedor MJ (2002) Curr Opin Struct Biol 12:289–295
64. DeRose VJ (2003) Curr Opin Struct Biol 13:317–324
65. Morrissey SR, Horton TE, DeRose VJ (2000) J Am Chem Soc 122:3473–3481
66. Kim N-K, Murali A, DeRose VJ (2005) J Am Chem Soc 127:14134–14135
67. Babcock DF, Herrington J, Goodwin PC, Park YB, Hille B (1997) J Cell Biol 136:833–844
68. Lehninger AL, Carafoli E, Rossi CS (1967) Adv Enzymol Relat Areas Mol Biol 29:259–320
69. Mccormack JG, Denton RM (1980) Biochem J 190:95–105
70. Gunter TE, Gunter KK, Sheu SS, Gavin CE (1994) Am J Physiol 267:C313–C339
71. Carafoli E (2003) Trends Biochem Sci 28:175–181
72. Saris NE (1963) Scientiarum Fennica Commentationes Physico Mathematicae 28:3–59
73. De Luca M, Engstrom G (1961) Proc Natl Acad Sci USA 47:1744–1747
74. Vasington FD, Murphy JV (1962) J Biol Chem 237:2670–2672
75. Murphy AN, Bredesen DE, Cortopassi G, Wang E, Fiskum G (1996) Proc Natl Acad Sci USA 93:9893–9898
76. Kluck RM, Bossy-Wetzel E, Green DR, Newmeyer DD (1997) Science 275:1132–1136
77. Peebles CL, Perlman PS, Mecklenburg KL, Petrillo ML, Tabor JH, Jarrell KA, Cheng HL (1986) Cell 44:213–223
78. Shannon RD (1976) Acta Crystallogr A 32:751–767
79. Martin RB (1986) Met Ions Biol Syst 20:21–65
80. Morf WE, Simon W (1971) Helv Chim Acta 54:794–810
81. Sigel H, Massoud SS, Corfù NA (1994) J Am Chem Soc 116:2958–2971
82. Sigel H, Griesser R (2005) Chem Soc Rev 34:875–900
83. Moreno-Luque CF, Griesser R, Ochocki J, Sigel H (2001) Z Anorgan Allgem Chem 627:1882–1887
84. Sigel H, Massoud SS, Tribolet R (1988) J Am Chem Soc 110:6857–6865
85. Scheller KH, Abel THJ, Polanyi PE, Wenk PK, Fischer BE, Sigel H (1980) Eur J Biochem 107:455–466
86. Muranyi A, Finn BE (2001) In: Bertini I, Sigel A, Sigel H (eds) Handbook on metalloproteins. Marcel Dekker, New York, pp 93–152
87. Irving HM, Williams RJP (1953) J Chem Soc 3192–3210
88. Grosshans CA, Cech TR (1989) Biochemistry 28:6888–6894
89. Kazakov S, Altman S (1991) Proc Natl Acad Sci USA 88:9193–9197
90. Giannakis C, Forbes IJ, Zalewski PD (1991) Biochem Biophys Res Commun 181:915–920
91. Stano NM, Chen J, McHenry CS (2006) Nat Struct Mol Biol 13:458–459
92. Sigel RKO, Sigel H (2007) Met Ions Life Sci 2:109–180
93. Travers KJ, Boyd N, Herschlag D (2007) RNA 13:1205–1213
94. Rode BM, Schwenk CF, Hofer TS, Randolf BR (2005) Coord Chem Rev 249:2993–3006
95. Baes CF Jr, Mesmer RE (1976) The hydrolysis of cations. Krieger, Malabar
96. Helm L, Merbach AE (1999) Coord Chem Rev 187:151–181
97. Lincoln SF (2005) Helv Chim Acta 88:523–545
98. Inada Y, Mohammed AM, Loeffler HH, Funahashi S (2005) Helv Chim Acta 88:461–469
99. Lincoln SF, Merbach AE (1995) Adv Inorg Chem 42:1–88
100. Sigel H, Martin RB (1994) Chem Soc Rev 23:83–91